AIAA JOURNAL
Vol. 38, No. 6, June 2000

Size Effects in Scaled Fiber Composites Under Four-Point Flexure Loading

David P. Johnson*
Mississippi State University, Mississippi State, Mississippi 39762
John Morton†
Royal Aerospace Establishment, Farborough, Hampshire, England GU14 6TD, United Kingdom
Sotiris Kellas‡
Lockheed Engineering and Sciences Company, Inc., Hampton, Virginia 23681-0001
and
Karen E. Jackson§
U.S. Army Research Laboratory, Hampton, Virginia 23681-0001

The effect of specimen size on the four-point flexural response of ply-level and sublaminate-level scaled composites was investigated. Two laminates were studied, namely, $[+45/-45/+45/-45]_s$ and $[+45/-45/0/90]_s$. The material system used was AS4/3502 graphite/epoxy. Enhanced x-ray radiography and edge photomicroscopy were used to examine damage development in specimens loaded to various fractions of their ultimate load. This nondestructive examination was coupled with observations of the load/deflection response to try to correlate scaling effects with the damage development in the specimens. Results were compared to previous studies involving tensile scaling effects. It was found that the strength of ply-level scaled laminates decreased as specimen size increased, and that this effect was modeled well using the typical fracture mechanics scaling law. Sublaminate-level scaled specimens did not show a pronounced scaling effect. Although there seemed to be a slight decrease in strength with increased specimen size, the effect was small and may not be statistically significant.

Introduction

FOR advanced composite materials to be more widely used for structural applications, it is necessary to understand the nature of changes in mechanical behavior as composite laminates are scaled in size. To reduce production costs, full-scale structures are typically designed using small-scale coupon and/or scale-model testing. These results must then be used to predict the behavior of the full-scale part. It is necessary, therefore, to know whether composite materials show any scaling effect or size effect, which can be defined as any deviation, with changing size, in the mechanical response of a material from some accepted law of mechanics.

As an example, it is well known that brittle materials, such as glass and ceramics, exhibit scaling effects in quasi-static tension.[1] Although they are not classical brittle materials, in that cracks do not propagate in a self-similar manner, composites do display brittle failure mechanisms. Hence, it is of interest to know whether composites also demonstrate scaling effects.

Background

Research has been done (for example, see Refs. 2–12) to investigate scaling effects in unidirectional and laminated composites. In general, investigators have found that unidirectional composites show a decrease in specimen strength with increased size. Wisnom[4] tested eccentrically loaded columns. He postulated that scaling effects in compression were more pronounced than those in tension, as his specimens changed failure mode from tensile in the small-scale specimens to compressive in the larger ones.

Scaling of laminates involves special considerations, such as the method of scaling the laminate thickness. Because similitude cannot be satisfied exactly, one can increase the thickness of a given laminate by simply grouping together additional plies of the same orientation (so-called ply-level scaling). This method has been shown to reduce the strength of specimens containing large numbers of blocked plies.[5,6]

Alternatively, one can increase the thickness of scaled laminates by repeating a given sublaminate (so-called sublaminate-level scaling). This method has the advantage that groups of plies of the same orientation need not be blocked together, but suffers in that similitude is not maintained. In-plane extensional and shear stiffnesses, as well as Poisson's ratio, are independent of scaled thickness, but out-of-plane (bending and twisting) stiffnesses are not. Figure 1 illustrates the two methods of thickness scaling.

In simple tensile tests, ply-level scaled laminates have been shown to exhibit significantly decreased strengths as specimens are increased in size. However, scaling effects in sublaminate-level scaled specimens have been shown to be much less pronounced, unless the baseline specimens delaminate (which would be avoided in a practical design anyway).

Flexure Scaling

One of the most critical properties in composite design is the compressive behavior. With the desire to move from tensile properties to an investigation of compressive properties, the determination was made to study the response of scaled coupons loaded in flexure, which involves a combination of tensile and compressive loading. Four-point flexure loading was chosen to minimize the influence of through-the-thickness shear stresses on the response.

Classical lamination theory (CLT) and simple beam theory indicate that the bending stiffnesses of ply-level scaled specimens of a given laminate stacking sequence should be independent of size. Bending stiffnesses of sublaminate-level scaled coupons may increase or decrease in larger scaled specimens, depending on the stacking sequence. However, currently used failure criteria still suggest that the ply failure stress and strain should be independent of size.

Therefore, to investigate scaling effects in laminated composite coupons loaded in four-point flexure, two baseline stacking sequences and two methods of scaling were chosen, namely, $[\pm 45/\pm 45]_s$ and $[\pm 45/0/90]_s$ using ply- and sublaminate-level

Received 9 September 1998; revision received 28 February 1999; accepted for publication 13 September 1999.

*Assistant Professor, Department of Aerospace Engineering, Mail Stop 9549.
†Director, Structural Materials Centre, Defence Research Agency.
‡Principal Engineer, Mail Stop 371, NASA Langley Research Center, 144 Research Drive.
§Aerospace Engineer, Vehicle Technology Center, Mail Stop 495, NASA Langley Research Center. Associate Fellow AIAA.

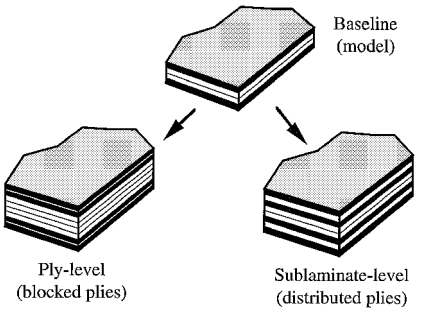

Fig. 1 Sublaminate- vs ply-level scaling of thickness.

scaling. Scaled sizes included doubling and quadrupling the baseline size ($n = 1, 2, 4$)

Strain gauges were used throughout the study to obtain top and bottom longitudinal laminate strains, and the load and crosshead displacement were recorded directly from the testing machine. Enhanced radiography and optical microscopy were used to evaluate damage processes and modes of failure. Characteristic response curves for the different sizes were normalized and compared for each laminate stacking sequence, and observed damage processes were correlated with specific features on the stress/strain curves.

Analytical Methods

Two particular models have been used when describing the scaled response of unidirectional composites. These models will be presented and discussed.

In addition to comparing the strain to failure and strength data to existing models for scaled response, it was hoped that the load/deflection curves could be used to identify damage initiation and propagation during the tests. To this end, a model had to be developed to describe the load/deflection response of the specimens loaded in flexure.

In a tensile test, if the material properties of the specimen remain linear to failure (as laminated composites essentially do), the stress/strain response will also be linear. Hence, the observation of the specimen's response and, in particular, noting the onset and magnitude of nonlinearities present yield certain information about the initiation and propagation of damage in the specimen. It was anticipated that a similar technique could be employed with the flexure specimens. However, because of the geometry of the test fixture, and because the deflections were too large for the application of small deflection beam theory, the load/deflection response was slightly nonlinear throughout the range of the tests.

Prediction of Elastic Load/Deflection Response

Several factors contributed to nonlinear elastic load/deflection response of specimens in the fixture. A computer code[11] was written in order to model each of these factors and to predict the nonlinear response of a linearly elastic specimen.

All of the sources of nonlinear elastic behavior were because deflections and slopes in the specimens were not small. One of the things this influences is the beam bending equation. The linearized form of this equation is no longer valid. The nonlinear bending equation can be expressed as[13]

$$\frac{\mathrm{d}^2 y}{\mathrm{d}x^2} = \frac{M}{EI}\left[1 + \left(\frac{\mathrm{d}y}{\mathrm{d}x}\right)^2\right]^{\frac{3}{2}} \tag{1}$$

After all geometry was defined, including the rollers and the specimen, a no-penetration boundary condition was enforced between the specimen and the rollers. The computer code then employed a fourth-order Runga–Kutta routine, in combination with Euler's method, to solve for the shape of the beam, given the displacement of the middle rollers and the bending stiffness.

A second source of elastic nonlinearity comes from the measurement of force by the testing machine. Even modeling friction in the bearings of the fixture, the load is always applied nearly normal to the surface of the specimen. Nevertheless, only the vertical component of this force is recorded by the testing machine's load cell.

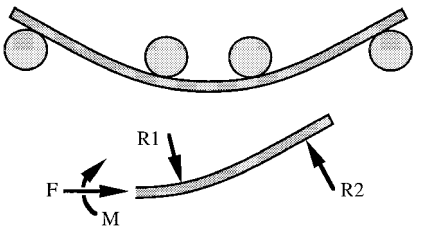

Fig. 2 Small compressive axial force F required for equilibrium for large deflections.

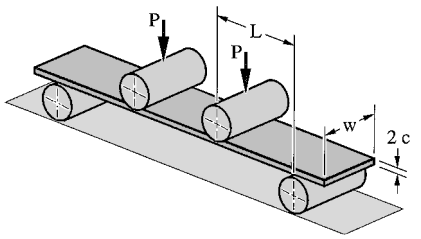

Fig. 3 Load and geometric quantities of Eq. (2).

When the deflected slope of the specimen grows large, this vertical component of the force can be significantly different from the actual force being applied by the roller.

In addition, as the specimen deflects, the position of contact between the rollers and the specimen changes. This affects the moment that a given force produces.

Finally, one more source of elastic nonlinearity was considered. This nonlinearity did not affect the load/deflection curve, but rather the load/strain response. Figure 2 shows a representative specimen in a four-point bend fixture and a free-body diagram of a portion of the specimen. Because the two roller forces in the free-body diagram are not parallel, some axial force exists in the gauge section. This is because although the vertical components of these forces are equal, the horizontal components are not. Normally beams are not loaded axially because all loads are assumed to be transverse. Although this is not the case with the flexure specimens tested in this work, the effect was found to be negligible compared to the bending loads, and the surface strains were not appreciably affected.

The variables input to the code included the geometry of the specimen and the fixture, the bending stiffness of the specimen, the extensional stiffness of the specimen, and the coefficient of friction between the rollers and the specimen.

The output of the code included the vertical load component, crosshead displacement, top and bottom surface strains, and gauge section moments.

Normalization

Because the responses of different sizes of flexure specimens cannot be directly compared, some method of normalization was needed. A natural way to do this would be to simply remove any geometrically dependent terms. Let us consider the strain in the outer fibers of the beam. Even though deflections may be large during part of the tests, for the purposes of normalization, consider the strain during small deflections. This can be expressed as

$$\varepsilon = PLc/E_b I \tag{2}$$

where P is the load applied by one roller; L is the distance between inner and outer rollers; and c, E_b, and I are the specimen's half-thickness, bending stiffness, and second moment of area of the cross section.

The load as well as the geometric quantities in Eq. (2) are shown in Fig. 3. The second moment of area of the cross section is simply $(\frac{2}{3})wc^3$.

All dimensions of the specimens are scaled simultaneously, so that in Eq. (2) the length L, the half-thickness c, and the second moment of area I are scaled as follows:

$$L = nL^*, \qquad c = nc^*, \qquad I = n^4 I^* \tag{3}$$

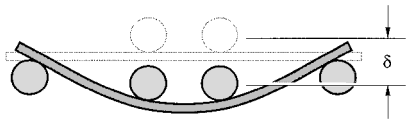

Fig. 4 Schematic showing the deflection of the rollers δ.

where L^*, w^*, and c^* are the dimensions of the baseline specimens, and $n = 1, 2, 4$. Recognize that the scaled deflection will be

$$\delta = n\delta^* \tag{4}$$

where the deflection δ is the distance the inner rollers travel, as seen in Fig. 4.

Substituting Eqs. (3) into Eq. (2) and rearranging Eq. (4) yields

$$\varepsilon = \frac{PL^*c^*}{n^2 E_b I^*}, \qquad \delta^* = \frac{\delta}{n} \tag{5}$$

Equations (5) give the correct order of the scaling factor n to be used in the normalization process. Hence, the normalized equations for the load and deflection are taken simply as

$$\Pi = P/n^2 E_b, \qquad \Delta = \delta/n \tag{6}$$

where Π and Δ are the normalized load and deflection, respectively. The bending stiffness E_b was used in the normalization process because, according to CLT, it will vary for each sublaminate-level scaled specimen size. This collapses the elastic responses of all specimens with the same scaled outer-to-inner roller span ratios onto the same curve, so that differences in response can be readily compared.

Failure Prediction

Numerous approaches for modeling scaling effects in composites have been developed, most of which reduce to two similar equations. The fracture mechanics approaches lead to equations of the form[14]

$$S/S_b = 1/\sqrt{n} \tag{7}$$

where S and S_b are the strengths of the scaled and baseline sizes, respectively, and n is the scaling factor. Note that this approach relies on an existing crack propagating in a self-similar manner. Because failure modes in composites are more complex than in quasi-homogeneous materials, self-similar crack propagation may not occur in composites. However, the model has been used to describe failure in unidirectional and ply-level scaled composites. The applicability of this model to sublaminate-level scaling is less clear because similitude between the scaled and the baseline sizes is not maintained in the stacking sequence.

The other approach that has found use is the Weibull statistical model. This states that the strength of a specimen can be expressed as

$$\ln S(V) = C - (1/m)\ln V \tag{8}$$

where $S(V)$ is the strength of the specimen, C is a constant, m is a constant (the so-called Weibull modulus), and V is the volume of the specimen.

For application to ply-level scaling, Eq. (8) reduces to the following:

$$S/S_b = (V_b/V)^{1/m} \tag{9}$$

The volume ratio can be related to the scaling factor n, and Eq. (9) can be written as

$$S/S_b = 1/n^{3/m} \tag{10}$$

The Weibull modulus m can be approximated[15] as

$$m \approx 1.2/\mathrm{CV} \tag{11}$$

where CV is the coefficient of variation of the strength data. A CV of 20%, therefore, would make Eqs. (7) and (10) equivalent.

Experimental Procedure

Specimens

Two baseline layups and two scaling methods were chosen for this study, as well as three specimen sizes. In the discussion that follows, each laminate type will be referred to by the stacking sequence of its baseline specimen. The stacking sequences for the three sublaminate- and ply-level scaled laminates were as follows: baseline stacking sequence $[+45/-45/0/90]_{2s}$, sublaminate-level scaled $[+45/-45/0/90]_{2ns}$, ply-level scaled $[+45_n/-45_n/0_n/90_n]_{2s}$, baseline stacking sequence $[+45/-45/+45/-45]_{2s}$, sublaminate-level scaled $[+45/-45/+45/-45]_{2ns}$, and ply-level scaled $[+45_n/-45_n/+45_n/-45_n]_{2s}$, where $n = 1$, 2, or 4.

The in-plane dimensions of the specimens were chosen to be $(12.5)n \times (75)n$ mm where $n = 1$, 2, or 4. In the present work, specimen groups are referred to by the scaling factor n and the method of scaling. Thus, a specimen referred to as $2p$ is a ply-level scaled $n = 2$ specimen. A specimen referred to as 1 (no scaling method) is a baseline specimen.

A cross-ply stacking sequence was also fabricated and tested. However, failures tended to be at the rollers, not in the gauge section. The inclusion of a compliant shim between the rollers and the specimens eliminated the problem, but not enough coupons remained to gain statistically reliable data.

All panels were fabricated from AS4/3502 graphite/epoxy unidirectional prepreg and were autoclave cured following the manufacturer's recommended cycle. Following fabrication, each panel was C-scanned to assess quality. All coupons were cut using a water-cooled diamond saw and were stored at nominal room conditions.

Fixture

A set of four-point flexure fixtures was designed and built for the tests. The inside and outside roller spans were $25n$ and $57n$ mm, respectively. The roller diameters were $12.5n$ mm. Each roller was mounted in brackets containing ball bearings to minimize friction. Care was taken to allow for precise geometric scaling of the moment arms, roller diameters, and the brackets holding the rollers.

Mechanical Testing

Of each specimen size and laminate stacking sequence, at least five coupons were tested to failure. Typical load/deflection response was then examined, and points of interest were identified. The remaining specimens of each type were then loaded to different proof loads, corresponding to these points of interest. These preloaded specimens were then removed from the fixture and examined for damage using nondestructive techniques.

Load and crosshead displacement were recorded directly from the testing machine, and top and bottom longitudinal strain was recorded using longitudinal foil-type strain gauges. The crosshead speed was varied with the specimen gauge length to yield approximately equivalent strain rates.

Damage Evaluation

Preloaded specimens were examined using two nondestructive techniques. These were penetrant-enhanced x-ray radiography and optical microscopy.

X-Ray Radiography

Preloaded specimens were soaked in an x-ray-opaque zinc iodide dye penetrant solution. Contact exposures were then made to yield radiographs of the damage in each preloaded specimen. Some of the specimens, in which damage was minimal or nonexistent, were reloaded after the x-ray process. To minimize the effect of the zinc iodide solution on the behavior of the composite material, these specimens were reloaded again within a day or two.

Optical Microscopy

After loading, the edges of the specimens were polished using 1-μm aluminum oxide powder. The specimen edges were then examined and photographed using an optical microscope. These micrographs were used to locate the plies in which damage occurred. Damage sites seen on the radiographs could then be directly

compared with optical micrographs of the same region of the specimen edge to better characterize the damage.

Results and Discussion

Because of the anisotropic nature of laminated composite materials, some bend/twist coupling exists in the specimens. This coupling is most pronounced in the baseline and ply-level scaled specimens and becomes less pronounced with increased sublaminate-level scaled size. CLT indicates that even for the baseline and ply-level scaled specimens, these coupling terms are small compared to other stiffness terms. It was assumed, therefore, that the coupled response had a negligible effect on the results.

The following is a presentation of the results, starting with a comparison of the observed vs predicted load/deflection response.

Load/Deflection Predictions vs Experiment

To establish that the predicted elastic response was representative of reality, two isotropic specimens were tested for comparison. The first was an aluminum specimen that yielded at a deflection that was significantly below that observed in the composite coupons. Therefore, a polymeric [poly(methyl methacrylate); PMMA] specimen was tested. Figures 5 and 6 show the actual load/deflection curves for the aluminum and PMMA specimens, compared to the predicted elastic response. The purpose of the comparison was to validate that the computer code could predict the effective stiffness and nonlinear elastic structural response of a coupon made of linear elastic material. No failure is predicted.

Other than the fixture and specimen geometry, the only input needed was the bending stiffness of the coupon. For isotropic specimens, the product of the extensional stiffness E and the moment of inertia I constitutes the bending stiffness. The extensional stiffness of the aluminum was acquired from published literature, and the stiffness of the PMMA specimen was obtained by a simple tension test.

Note in Fig. 5 that the early portion of the aluminum specimen's load/deflection curve is predicted well, but that plastic yielding occurred relatively early in the response. Figure 6 shows that the PMMA specimen also followed the predicted curve for a significant portion of its response. The deviation in the latter portion of the response is due to plastic yielding of the PMMA. Permanent deformation was observed in the specimens on unloading. Hence, deviation from the predicted response indicates nonlinear material behavior.

Again, recall that the only input data for the predicted curves were the specimen and fixture geometry and the bending stiffness EI.

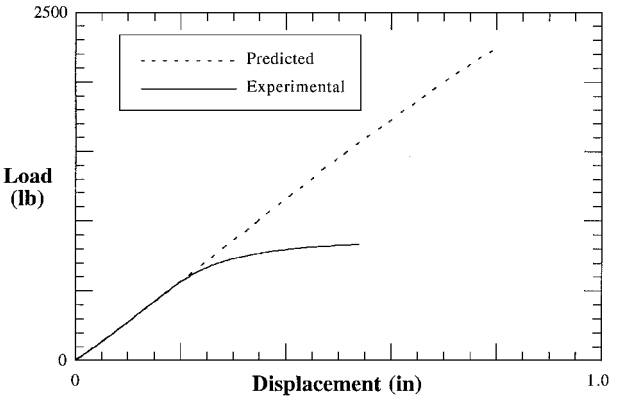

Fig. 5 Predicted vs experimental load/deflection plot: aluminum specimen.

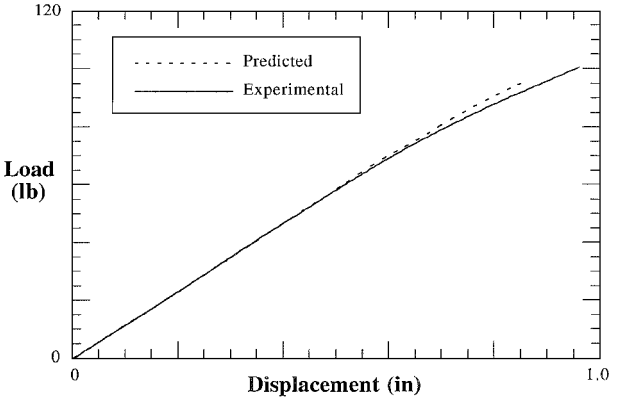

Fig. 6 Predicted vs experimental load/deflection plot: PMMA specimen.

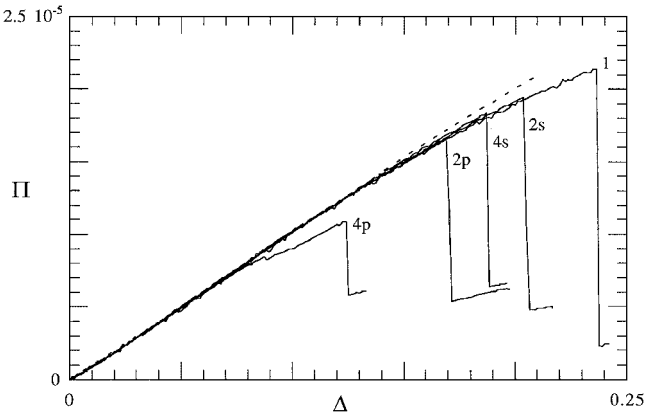

Fig. 7 Normalized response of $[\pm 45/0/90]_{2s}$ specimens.

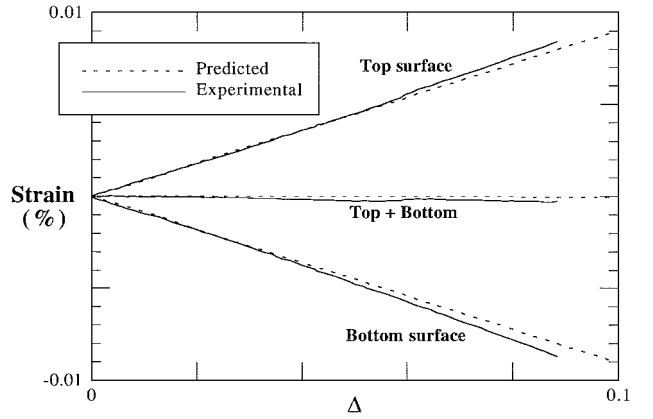

Fig. 8 Top and bottom strains vs predictions.

Normalized Load/Deflection Response

Equations (6) were used to normalize the response of specimens of different sizes. Here, the bending stiffnesses for the composite specimens was initially predicted by CLT. However, it turned out that these predictions were often in error by as much as 15–20%. Therefore, measured bending stiffnesses were used in the normalization process.

$[\pm 45/0/90]_{2s}$ Specimens

Figure 7 shows the normalized response of typical specimens from each size and scaling method. They are labeled according to the scaling factor n and the scaling method. Thus, the curve labeled $4p$ is a 64-ply, 50 × 300 mm, ply-level scaled specimen. The $n = 1$ specimens, of course, have no scaling method designated. All specimens failed catastrophically on the tensile side. Some delamination was present on the tensile side, most notably on the $4p$ specimens. This damage will be described in more detail later.

The dashed line is that predicted for a linear, elastic specimen. Note that the response does vary from the prediction. That this is caused by material nonlinearity is born out by the strain gauge readings. Figure 8 compares the top and bottom strain gauge readings for an $n = 1$ specimen, along with the sum of the strains, to their predicted values.

Unfortunately, due to matrix cracking in the tensile side surface plies, the strain gauges tended to fail at deflection levels that were

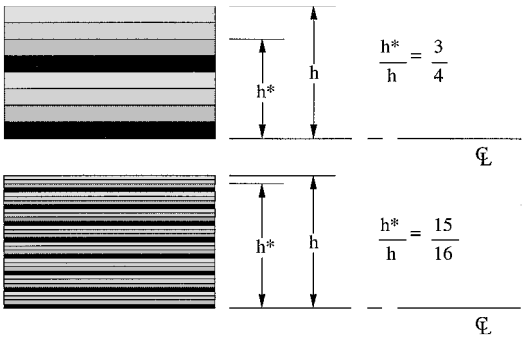

Fig. 9 Variation in relative position of the outermost 0-deg ply, in the $[\pm 45/0/90]_{2s}$ specimens, with sublaminate-level scaled size: top is baseline 1, and bottom is 4*s*.

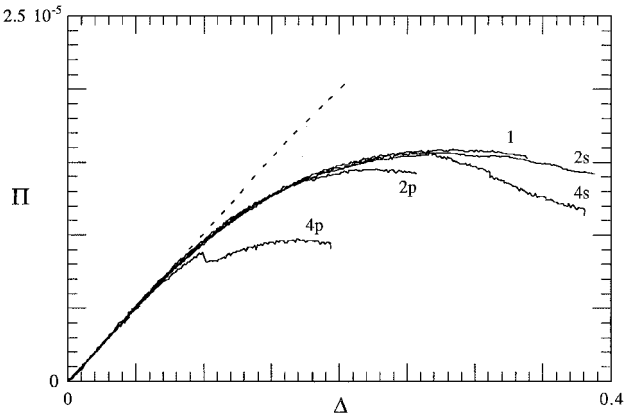

Fig. 10 Normalized response of $[45/-45/45/-45]_{2s}$ specimens.

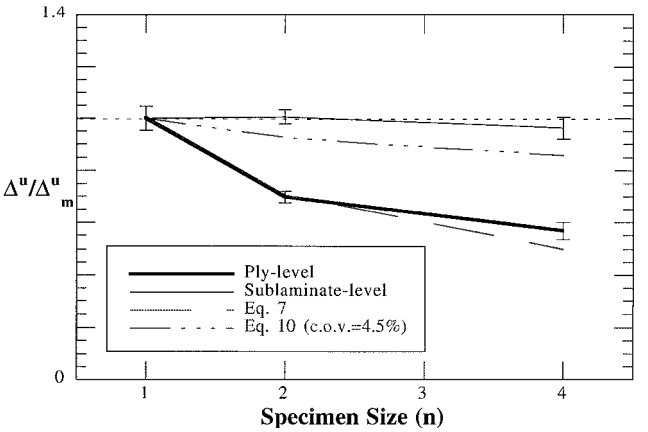

Fig. 11 Corrected (see text), normalized deflection at failure of $[45/-45/0/90]_{2s}$ specimens.

significantly below ultimate values. However, even at $\Delta = 0.1$, the strain at the midplane is shifting toward negative values. This is because of the well-known nonlinear behavior of composites, which tend to soften with increased strain in compression. Matrix cracks in the tensile 90-deg plies also tended to cause strain softening in the tensile side of the laminates, leading to a general strain softening of the laminate. It can be seen in Fig. 8 that the strain softening in the compressive plies is more pronounced than the strain softening due to damage in the tensile plies.

Observing Fig. 7, it can be seen that, with the exception of the 4*p* specimens, all specimens followed the same general load/deflection curve. There is a significant decrease in ultimate load and deflection with increased scaled size for both scaling methods. Note, however, that the relative location of the 0-deg plies changes with varying size in the sublaminate-level scaling method. Figure 9 shows the location of the outermost 0-deg plies in the baseline and both ply-level scaled sizes compared to that of the 4*s* specimens. The ratio of the location of the outermost 0-deg ply to the location of the surface ply is $\frac{3}{4}$ for ply-level scales specimens vs $(4n-1)/(4n)$ for sublaminate-level scaled specimens.

Because all $[\pm 45/0/90]_{2s}$ specimens failed catastrophically when the outermost tensile 0-deg plies failed, the relative shift of those plies with increased sublaminate-level scaled size would affect the ultimate load and deflection. Specimens of this layup have outermost 0-deg plies that move relatively closer to the surface with increased sublaminate-level scaled size. This would mean that, for the same normalized load and deflection, the outermost 0-deg plies in larger sublaminate-level scaled specimens would experience strain that was greater in proportion to the relative shift in location. Hence, larger sublaminate-level scaled specimens fail at a lower normalized load and deflection.

$[45/-45/45/-45]_{2s}$ Specimens

Figure 10 shows the normalized load/deflection response for the ±45-deg specimens. With the exception of the 4*p* group, these specimens did not experience a catastrophic failure, and so the tests were arbitrarily stopped some time after the peak load was reached. The 4*p* group of specimens experienced sudden delamination of the tensile surface plies, associated with a distinct drop that can be noted in the load/deflection curve. After this initial delamination, the specimens continued to deflect in a manner similar to the other specimens. The test was stopped after a peak load was reached.

Average Δ at Failure Plots

Remember that although the load/deflection plots presented give a general idea of the shape of the response for the different specimens, they do not represent averages of all specimens of a given group. Rather, they represent the response of a single typical specimen from each group. In this section, average deflection to failure plots will be presented.

$[\pm 45/0/90]_{2s}$ Specimens

Figure 11 shows the average deflection at failure. The error bars indicate one standard deviation in the data. For these specimens, the displacement at failure was modified according to the observation made previously concerning the changing relative position of the outermost 0-deg plies. Before normalization with respect to the baseline size, the deflection at failure for all sublaminate-level scaled specimens was multiplied by $(4n-1)/(4n)$ (see Fig. 9 and the accompanying commentary). In practice, this modification to the failure deflection renders it proportional to the strain of the outermost 0-deg plies. This is done so that failure strain in these plies can be compared between different sizes and scaling methods.

Plotted with the ply- and sublaminate-level scaled data in Fig. 11 are Eqs. (7) and (10). The Weibull modulus, needed for Eq. (10), can be related to the coefficient of variation through Eq. (11). A coefficient of variation of 4.5% was used as a representative value for the variability of the data seen in specimens of this layup.

$[45/-45/45/-45]_{2s}$ Specimens

Because these specimens did not fail catastrophically, deflection at failure was defined as the deflection at which the load reached its maximum value. Figure 12 shows its variation with respect to specimen size. Again, the error bars represent one standard deviation in the data. It can be seen that the scatter of these data is significantly lower than for the previous specimens. A coefficient of variation of 2.5% was used for finding the Weibull modulus in Eq. (11).

Note that Eq. (7), which was developed using fracture mechanics, predicts the ply-level scaled results relatively well. The change in failure mode to a delamination of the tensile surface plies for the 4*p* specimens (recall Fig. 10) accounts for their unusually low average failure.

General Discussion of Load/Deflection

As has been reported in the literature for tensile loading,[5,6] ply-level scaling leads to reduced strain to failure with increased specimen size.

When delamination is not present, sublaminate-level scaling has been reported as having no significant effect on failure for $n = 1-4$

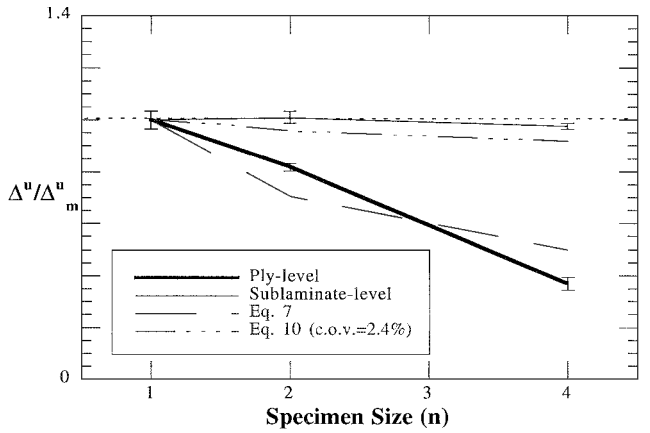

Fig. 12 Normalized deflection at failure of $[45/-45/45/-45]_{2s}$ specimens.

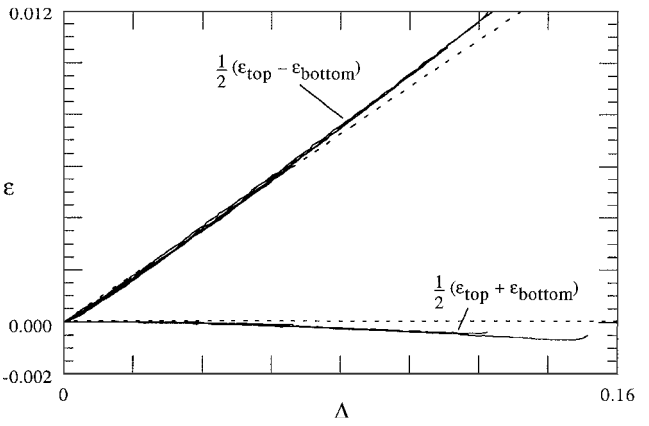

Fig. 13 Strain on top and bottom specimen surfaces vs normalized deflection of $[\pm 45/0/90]_{2s}$ specimens.

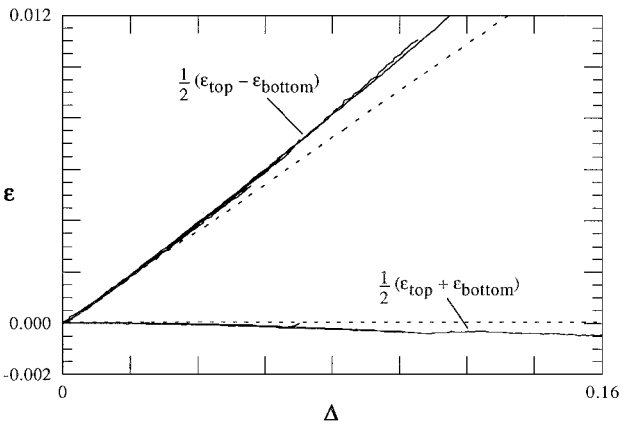

Fig. 14 Strain on top and bottom specimen surfaces vs normalized deflection of $[45/-45/45/-45]_{2s}$ specimens.

(Ref. 10). Yet it must be remembered that a quadrupling in size does not represent a large change in specimen volume. Indeed, structures may be orders of magnitude larger than the coupons used to secure design data. For this reason, larger sublaminate-level scaled specimens must be used in the future to further investigate possible scaling effects. It does seem possible, viewing Figs. 11 and 12, that a slight weakening effect, with larger sizes, may be present in sublaminate-level scaled specimens.

As far as modeling scaling effects is concerned, although the fracture mechanics model predicts ply-level scaling well, it cannot predict the response of sublaminate-level scaled specimens. This is because of the violation of similitude that sublaminate-level scaling represents. Self-similar damage is not allowed in sublaminate-level scaled specimens.

The Weibull statistical model of Eq. (10) seeks to account for scale effects due only to the statistical variability of the data. Larger scaling effects are predicted for data with a higher degree of scatter. However, with the low variability in the current data, the Weibull approach still overstates any scaling effect in the sublaminate-level scaled specimens. It does not fit ply-level scaling data at all.

This is most probably because the Weibull model is a weak link model. Once a fiber has broken, it is assumed to no longer contribute to load sharing. This is clearly not the case with composites, as broken fibers can be reloaded on failure. However, some have applied this model to composite scaling effects studies in the past.

One last considerationis the manner in which the roller deflection was obtained. It was assumed that the roller deflection was identical to the crosshead displacement of the testing machine. Although this is only true if the testing machine and crosshead are infinitely stiff compared to the specimen, some observations can be made. The crosshead deflection δ has two components:

$$\delta = \delta^* + P/k \tag{12}$$

where δ^* is the actual deflection of the rollers, P is the force applied to the specimen, and k is the stiffness of the testing machine and crosshead.

Taking into account the normalization of the load and deflection in Eq. (6), Eq. (12) can be solved for the normalized deflection of the rollers:

$$\Delta^* = \Delta - \Pi n(E_b/k) \tag{13}$$

This would represent a linear dependence of the actual displacement Δ^* on the scaled size n. However, the second term of the right-hand side of Eq. (13) is much smaller (it is of the order of 10^{-6}) than the crosshead deflection observed. For practical purposes, then, the offset can be neglected.

Normalized Strain/Deflection Response

In the response of all specimens, strain softening was observed. This strain softening was most pronounced on the compressive side, as can be seen in Fig. 8. It occurred before any detectable failure modes were present in the specimens. When failure (in the form of matrix cracks) began developing in the specimens, the strain gauges typically failed, ending the strain data. Figures 13 and 14 show plots of strain vs normalized deflection Δ for each of the laminates. The plots show both the average and the average magnitude, of the top (tensile) and bottom (compressive) strains. Dashed lines indicate the predicted values of each assuming linear elastic material behavior. Any deviation of the average strain from zero represents a shift in the neutral axis of the specimen. Any deviation of the average magnitude of the strain from the predicted curve represents nonlinear material behavior.

Each of Figs. 13 and 14 contains the strain/deflection response of one typical specimen from each size group and scaling method (1, $2p$, $2s$, $4p$, $4s$). Although the two laminates differed from one another in their amount of strain softening and neutral axis shifting, all specimens from a given laminate behaved identically.

Each laminate has a different characteristic response. Although all laminates experienced shifting of the neutral axis of approximately the same magnitude, they showed different amounts of strain softening.

Damage

For a given layup, damage in the sublaminate-level specimens developed in a similar manner in all sizes of specimens. However, the ply-level specimens tended to change failure mode in the larger specimens. Figures 15–18 are schematic diagrams representing in-plane x radiographs and edge photomicrographs. Schematics of micrographs have labels marking the plies through the thickness, as well as an indication of the magnification at which the specimen is being viewed. This is important because the $4p$ specimens are viewed at lower magnification than the others.

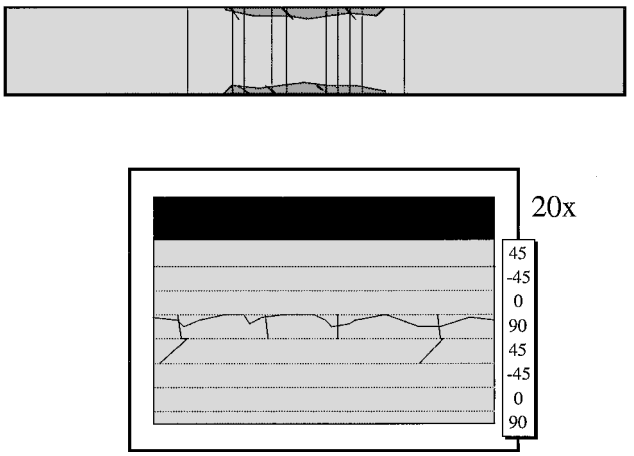

Fig. 15 Typical development of damage in 1, 2*s*, and 4*s* $[\pm 45/0/90]_{2s}$ specimens.

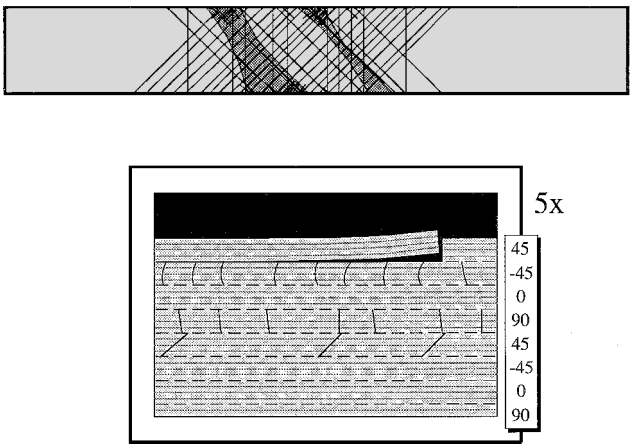

Fig. 16 Typical development of damage in 4*p* $[\pm 45/0/90]_{2s}$ specimens.

$[\pm 45/0/90]_{2s}$ Specimens

Quasi-isotropic sublaminate-level scaled specimens experienced first-ply failure as transverse matrix cracks in the 90-deg plies closest to the tensile surface. These cracks spanned the entire width of the specimens (Fig. 15).

At higher stress some of these 90-deg ply cracks propagated into the adjacent 45-deg plies. See the edge micrograph (bottom) in Fig. 15. In the radiograph (top) in Fig. 15 it can be seen that the cracks in the 45-deg plies did not propagate across the specimen width.

At still higher stress, a delamination formed in the outermost tensile 90-deg ply. This delamination propagated only a short way into the specimen width and did not significantly affect the bending stiffness.

The large ply-level scaled specimens 4*p* did not fail in the same manner as the sublaminate-level scaled specimens. Instead, these specimens experienced cracking and delamination in the tensile surface 45-deg plies. Figure 16 shows that these delaminations were associated with a surface crack and that they propagated through the width of the specimens. These large delaminations precipitated the early failure of the specimens that can be seen in Fig. 7. Recall that the edge view (bottom) in Fig. 16 represents a lower magnification than its counterpart in Fig. 15. Thus, it is the entire block of four 45-deg surface plies that is delaminating in Fig. 16.

$[45/-45/45/-45]_{2s}$ Specimens

Sublaminate-level scaled specimens of this layup experienced first-ply failure as matrix cracks in the surface 45-deg plies. These cracks then propagated into adjacent −45-deg plies, and so on. Figure 17 shows schematics of typical damage development. At some point in the response, delaminations formed in the surface plies. These delaminations did not propagate far into the specimen width,

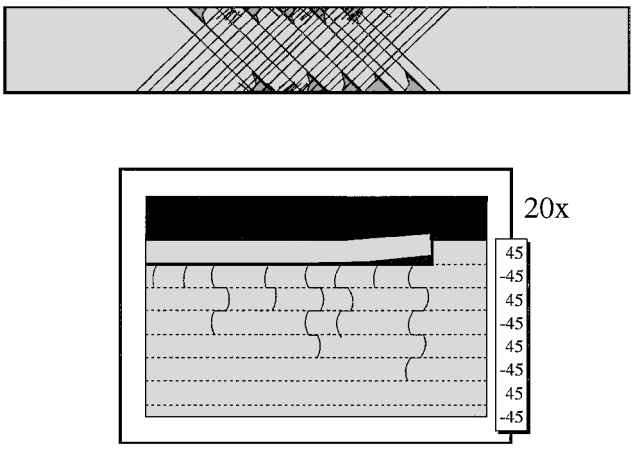

Fig. 17 Typical development of damage in 1, 2*s*, and 4*s* $[45/-45/45/-45]_{2s}$ specimens.

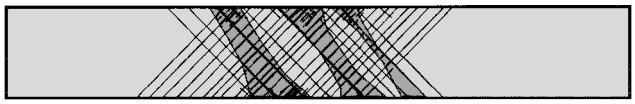

Fig. 18 Typical development of damage in 4*p* $[45/-45/45/-45]_{2s}$ specimens.

as seen in the x ray (top) in Fig. 17. The middle-sized ply-level scaled specimens 2*p* also showed damage development similar to this.

On the other hand, the large ply-level scaled specimens 4*p* experienced large delaminations similar to the 4*p* quasi-isotropic specimens (see Fig. 18). This large-scale delamination accounted for the premature failure of the 4*p* specimens shown in Fig. 10. Development of other damage modes (transverse ply cracking) was similar to that in the sublaminate-level scaled specimens.

Conclusions

Two baseline layups were tested in four-point flexure. These layups were $[45/-45/0/90]_{2s}$ and $[45/-45/45/-45]_{2s}$. Both ply-level and sublaminate-level geometric scaling were used, with the largest specimens being four times the size of the baseline specimens.

A set of scaled fixtures was used to test specimens in four-point bending. All of the specimens failed within the gauge section on the tensile side.

Both of these layups showed significant reductions in deflection at failure (and, hence, failure strain) when ply-level scaling was employed. These reductions were predicted well by the model developed using fracture mechanics [Eq. (7)]. The failure mode in the largest ply-level scaled specimens, $n = 4$, was significantly different from the failure mode of smaller specimens. In these large specimens, large delamination regions formed adjacent to matrix cracks in the block of four surface plies.

However, sublaminate-level scaled specimens of layups $[45/-45/45/-45]_{2s}$ and $[45/-45/0/90]_{2s}$, (when corrected to represent failure strain) did not show significant change in their failure deflections. Both layups showed about a 2–4% reduction in deflection at failure in the largest, $n = 4$, specimens, but this may not be statistically meaningful. Even larger specimens would have to be tested to confirm that a scaling effect in sublaminate-level scaled specimens does exist. The Weibull statistical model [Eq. (10)] is clearly not applicable to the ply-level scaled specimens and may not be applicable to sublaminate-level specimens either. Even with the low CV in the data, Eq. (10) overpredicts the magnitude of any scaling effect in ply-level scaled specimens.

Acknowledgments

This work was supported by the NASA Langley Research Center, under Contract NAS1-187471. Thanks are due to the Contract Monitor, Huey D. Carden.

References

[1]Timoshenko, S. P., *History of Strength of Materials*, McGraw-Hill, New York, 1953.

[2]Zweben, C., "The Effect of Stress Nonuniformity and Size on the Strength of Composite Materials," *Composites Technology Review*, Vol. 3, No. 1, 1981, pp. 23–26.

[3]Batdorf, S. B., "Note on Composite Size Effects," *Journal of Composites Technology and Research*, Vol. 11, No. 1, 1989, pp. 35–37.

[4]Wisnom, M. R., "Size Effects in Tensile, Compressive and Interlaminar Failure of Unidirectional Composites," *Proceedings of the ASME Annual Winter Meeting*, edited by G. J. Simitses, AD-Vol. 55, American Society of Mechanical Engineers, 1997, pp. 67–77.

[5]Kellas, S., and Morton, J., "Scaling Effects in Angle-Ply Laminates," NASA CR 4423, Feb. 1992.

[6]Jackson, K. E., "Scaling Effects in the Static and Dynamic Response of Graphite-Epoxy Beam-Columns," Ph.D. Dissertation, Dept. of Engineering Science and Mechanics, Virginia Polytechnic Inst. and State Univ., Blacksburg, VA, 1990.

[7]Kellas, S., and Morton, J., "Strength Scaling in Fiber Composites," NASA CR 4335, Nov. 1990.

[8]Morton, J., "Scaling of Impact-Loaded Carbon-Fiber Composites," *AIAA Journal*, Vol. 26, No. 8, 1988, pp. 989–994.

[9]Johnson, D. P., Felts, J. H., and Ho, M. T., "Scaling Effects in Composite Laminates Under Tensile, Flexural, and Compressive Loading," *Proceedings of the ASME Annual Winter Meeting*, edited by G. J. Simitses, AD-Vol. 55, American Society of Mechanical Engineers, 1997, pp. 59–66.

[10]Johnson, D. P., Morton, J., Kellas, S., and Jackson, K. E., "Scaling Effects in Sublaminate-Level Scaled Composite Laminates," *AIAA Journal*, Vol. 36, No. 3, 1998, pp. 441–447.

[11]Johnson, D. P., "The Effect of Specimen Size on the Mechanical Response of Laminated Composite Coupons Loaded in Tension and Flexure," Ph.D. Dissertation, Dept. of Engineering Science and Mechanics, Virginia Polytechnic Inst. and State Univ., Blacksburg, VA, 1994.

[12]Pheonix, S. L., Ibnabdeljalil, M., and Hui, C.-Y., "Size Effects in the Distribution for Strength of Brittle Matrix Fibrous Composites," *International Journal of Solids and Structures*, Vol. 34, No. 5, 1997, pp. 545–568.

[13]Popov, E. P., *Engineering Mechanics of Solids*, Prentice–Hall, Upper Saddle River, NJ, 1991.

[14]Atkins, A. G., and Caddell, R. M., "The Laws of Similitude and Crack Propagation," *International Journal of Mechanics Science*, Vol. 16, No. 8, 1974, pp. 541–548.

[15]Hitchon, J. W., and Phillips, D. C., "The Effect of Specimen Size on the Strength of CFRP," *Composites*, Vol. 9, 1978, pp. 119–124.

A. M. Waas
Associate Editor